CHEMICAL ENGINEERING TRANSACTIONS
VOL. 43, 2015
A publication of AIDIC
The Italian Association of Chemical Engineering
Online at www.aidic.it/cet
Chief Editors: Sauro Pierucci, Jiří J. Klemeš

ISBN 978-88-95608-34-1; **ISSN** 2283-9216
DOI: 10.3303/CET1543338

Catalytic Steam Reforming Pos-Gasification Using Toluene as Model Compound

Fernanda R. Silva*, Jornandes D. Silva

Polytechnic School - UPE, Laboratory of Environmental and Energetic Technology; Rua Benfica - 455, Madalena, Recife – PE, Brazil.
engmec_rodrigues@hotmail.com

The biomass gasification is gaining attention of scientists and researchers worldwide to be an innovative and efficient method for producing clean energy. While consuming 'junk' organic, such as sugarcane bagasse or rice husk, the gas produced in the process is used for heat or electricity generation (or gas turbine engines), synthesis of liquid fuels, hydrogen production, chemical synthesis and manufacturing of fuel cells. However, a key challenge in the development and improvement of the biomass gasification process is cleaning the gas produced in order to ensure its quality and applicability. Among the main impurities found in the gasification gas, the tar is one of the worst, the presence of this kind of impurity can prejudice the performance of the process and also damage equipment. There are several methods for tar removal. Catalytic process is the most studied and the one that shows the best results. This paper presents an isothermal mathematical model that characterizes production and consumption of tar, modelled by toluene, reforming reaction using nickel-based catalyst. A computer code in FORTRAN 90 language was developed to perform the simulation, which described the concentrations of the main components (C_7H_8, O_2, H_2 and CO), as well as the reaction yield and influence of temperature on generation of products. Then the optimum conditions for carrying out the process were determined.

1. Introduction

The concerns about using fossil fuels, the possible exhaustion of its sources and the environmental problems that the usage of this kind of energy source can cause are growing day by day, at the same time that the energetic demand is reaching the higher levels of the humanity history. Because of this, scientists and researchers have concentrated efforts on finding solutions to the current energy needs. These solutions are based on improvement and development of processes for energy generation from renewable sources. The biomass gasification is one of these renewable sources with a high potential for energy generation through the gasification, which will produce the synthesis gas that will be used to make biofuels, in fuel cells, gas turbines, or engines. The challenge in using biomass gasification for energy generation is the cleaning of the gas, since the produced gas contains a series of impurities.

Among the main impurities founded in the gas from biomass are ammonia, dust and tar. These kind of impurities can bring operating undesirable consequences, as blocking pipes due to condensation or polymerization of tar. Moreover, the burning of gases such as ammonia is a source of nitrogen oxides (Simmel et al., 1996).

Tar from biomass gasification is defined as hydrocarbons with molecular weight higher than benzene. There are several ways of removal this kind of impurity, two of them are the most used: selection of process conditions, known as primary methods, in which the operating conditions and the type of the reactor are selected, and the secondary methods, involving the use of cyclones, adsorbents, filters, riverbeds adsorption, scrubbers, electrostatic precipitators and catalytic removal (Quitete et al., 2014).

In view of the aim of this paper, the catalytic removal is the only method which will be addressed. The catalysts used on tar removal can be divided into two classes: mineral catalysts and synthetic catalysts. The main mineral catalysts are the dolomites, the olivines and the clay minerals and iron ores. The dolomites have

Please cite this article as: Rodrigues Silva F., Silva J.D., 2015, Catalytic steam reforming pos-gasification using toluene as model compound, Chemical Engineering Transactions, 43, 2023-2028 DOI: 10.3303/CET1543338

low costs and high efficiency, but low mechanical strength. The olivines have higher mechanical strength, but the efficiency is lower than the dolomites. The main synthetic catalysts are char, catalysts based on alkali metal, activated alumina and catalysts based on transition metals. Transition metals are considered to be good catalysts for steam reforming and dry methane and hydrocarbons. Catalysts based on nickel (Ni) supported on alumina, are cheaper and sufficiently active than other metals such as platinum (Pt), ruthenium (Ru) and rhodium (Rh) (Benedito, 2012).
In this paper an analysis of the behavior of temperature and concentrations of the main components of the tar from biomass gasification removal reaction in a fluidized bed catalytic reactor (FB) was done. Toluene was used as model compound because it's the main component of tar. The reaction yield and the influence of the temperature on it were also analyzed.

2. Mathematical Modeling

In this work, a kinetic model is presented, which is characterized by approach to chemical kinetics and transport phenomena involved. It is a model based on mass balances and energy of the solid and gaseous phases.
Mathematical models for catalytic fluidized bed reactors are important to design such systems starting from a laboratory scale, as well as starting from an existing system extrapolating them to the condition that it wants to use. A good model will help identify the sensitivity of performance of a catalytic reactor by varying different operating conditions and design parameters (Silva, 2013).

2.1. Kinetic Mechanism

For the present study the catalytic steam reforming of toluene reaction was considered:

$$2C_7H_8 + 7O_2 \xrightarrow{Ni\,/\,Al_2O_3} 8H_2 + 14CO \quad (1)$$

The component models of this reaction are defined as toluene (C_7H_8), oxygen (O_2), hydrogen (H_2) and carbon monoxide (CO). The stoichiometric coefficients models for these components are reported in Table (1).

Table 1: Stoichiometric coefficients of the reaction components

C_7H_8	O_2	H_2	CO
-2	-7	+8	+14

The reaction rate for each component of the reaction (1) is given by the following equation:

$$R_i = k_r C_i \quad (2)$$

Where: $R_i \rightarrow$ Reaction rate of component i [1/s]; $k_r \rightarrow$ Constant of reaction [-]; $C_i \rightarrow$ Concentration of component i [Kg m^{-3}].
The constant of reaction (k_r) is defined as:

$$k_r = k_{ro}\, exp\left(\frac{-Ea}{RT_g}\right) \quad (3)$$

Where: $k_{ro} \rightarrow$ Frequency factor [m/m^3]; Ea $\rightarrow$ Activation energy [KJ/Kg]; R $\rightarrow$ Universal gas constant [$m^3 \cdot Pa \cdot K^{-1} \cdot mol^{-1}$]; $T_g \rightarrow$ Gas temperature [K].
The consumption and formation net rates, r_i, for each component model of the reaction were obtained by using the following equation:

$$r_i = \sum_{j=1}^{n} v_{ij} R_j \quad (4)$$

Where: i = C_7H_8, O_2, H_2, CO; $r_i \rightarrow$ Net rate of the component i [mol s^{-1} m^{-3}]; $v_{ij} \rightarrow$ Stoichiometric coefficients of the reaction [-]; $R_j \rightarrow$ Reaction rate [1/s]; j = 1.
By using the equations (2), (3) and (4), we can obtain the net rate for each one of the components, as given in the table bellow:

Table 2: Net rate for each reaction component

Component	Net rate
C_7H_8	$r_t = -2K_{ro}\exp\left(\frac{-Ea}{RT_g}\right)C_{C_7H_8}$
O_2	$r_{O_2} = -7K_{ro}\exp\left(\frac{-Ea}{RT_g}\right)C_{O_2}$
H_2	$r_{H_2} = +8K_{ro}\exp\left(\frac{-Ea}{RT_g}\right)C_{H_2}$
CO	$r_{CO} = +14K_{ro}\exp\left(\frac{-Ea}{RT_g}\right)C_{CO}$

2.2. Model for the solid and gaseous phase

This paper seeks to analyze the concentrations of the individual components of the equation (1), thus, a model that is based on the conservation equations of mass was proposed, so that the generating terms are described by physical sub models (mass transfer) and chemicals (chemical kinetics). The mass balance equations of the reaction (1) model components (reactants and products) have been described as follows:
- Mass balance for the model components

$$h_i \frac{\partial C_i}{\partial t} + \frac{4Q_g}{\pi d^2}\frac{\partial C_i}{\partial z} = D_i \frac{\partial^2 C_i}{\partial z^2} + \varepsilon_s \eta_i r_i \tag{5}$$

- Initial and boundary conditions of the model components

$$C_i\big|_{t=0} = C_{t,0}\ ;\ D_i \left.\frac{\partial C_i}{\partial z}\right|_{z=0^+} = \frac{4Q_g}{\pi d^2}\left[C_i\big|_{z=0^+} - C_{i,0}\right];\ \left.\frac{\partial C_i}{\partial z}\right|_{z=l} = 0 \tag{6}$$

Where: i = C_7H_8, O_2, H_2, CO.
These equations are a simplified mathematical model of axial dispersion consisting of four partial differential equations (PDEs) and their respective initial and boundary conditions for a catalytic reactor FB. Due the axial dispersion have been considered, the boundary conditions are the Dankwerts conditions, that specify the gaseous and solid temperature values, and the model components concentration. The Method of Lines has been used for transforming the partial differential equations (PDEs) into ordinary differential equations (ODEs). A computer code in FORTRAN 90 language was developed in order to solve the system of ODEs and analyze the evolution of chemical species over time variable.

3. Results and discussion

Besides the analysis of the components concentration, it was also performed a study of the yield for hydrogen (H_2) and carbon monoxide (CO), which were analyzed according the following equations (Swierczynski, 2007):

$$\psi_{H_2} = \frac{(C_{H_2})_{out}}{8(C_t)_{in}}\ ;\ \psi_{CO} = \frac{(C_{CO})_{out}}{14(C_t)_{in}} \tag{7}$$

In the simulation of the process variables under study, the computational code was fed with the parameters reported in Table (3). In this table are shown the operating parameters of the catalytic reactor FB reaction area, mass transfer coefficients and physical properties of the gaseous and solid phases. The parameters of the Table (3) were obtained from experiments described in the literature and were admitted as fixed values.
Figure 1 shows the comparison between the experimental data obtained by Zhang et al. (2007) and the theoretical optimized data of the present study. The comparison shows a good fit of the experimental and optimized for the toluene conversion.
Figure 2 shows the production and consumption of the chemical species studied versus the time variable. H_2 and CO are produced from a initial values of C_{H2} = 0.00 Kg m^{-3} and C_{CO} = 0.00 Kg m^{-3} until reach the steady state in +- 35 s. The products are consumed from initial values of C_7H_8 = 0.142 and O_2 = 0.100, reaching their minimum values in +- 35 s.

Table 3: Input values of the operating conditions, properties of gas and solid phases used in the simulation (Oliveira, 2012)

Categories	Properties	Numerical Values
Operating Conditions	Gas operating temperature (T), ºC	800
	Pressure (P), atm	1.01
	Gas flow (Q_g), $m^3\ s^{-1}$	$1.367x10^{-6}$
	Initial concentration of C_7H_8 ($C_{C7H8,0}$), kg m^{-3}	0.142
	Initial concentration of O_2 ($C_{O2,0}$), kg m^{-3}	0.100
	Initial concentration of CO ($C_{CO,0}$), kg m^{-3}	0.000
	Initial concentration of H_2 ($C_{H2,0}$), kg m^{-3}	0.000
	Catalytic reactor diameter (d_r), m	0.032
	Catalytic reactor length (z), m	0.98
Gaseous phase properties	Diffusion coefficient of C_7H_8 ($D_{C7H8,0}$)	$2.571x10^{-5}$
	Diffusion coefficient of O_2 (D_{O2}), m^2s^{-1}	$3.24x10^{-5}$
	Diffusion coefficient of H_2 (D_{H2}), m^2s^{-1}	$3.52x10^{-5}$
	Diffusion coefficient of CO (D_{CO}), m^2s^{-1}	$4.61x10^{-5}$
Solid phase properties	Porosity of the solid phase (ε_s), (-)	0.39
Effectiveness factor	Effectiveness factor of reaction (η)	0.05

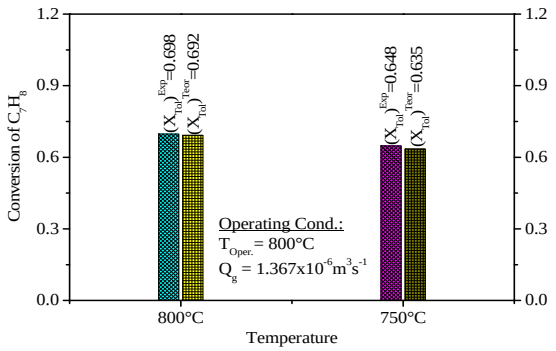

Figure 1: Comparison between the experimental data from Zhang et al. (2007) and the theoretical results of this paper. Where T is the temperature and Q_g is the gas flow.

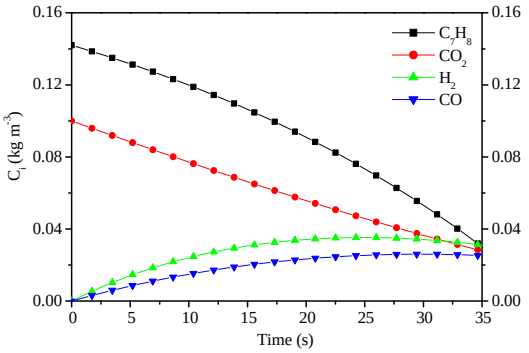

Figure 2: Concentration of the chemical species C_7H_8, CO_2, H_2 and CO over time variable under the following operating conditions: $Q_g = 1.367x10^{-6}\ m^3\ s^{-1}$ e T = 800 ºC.

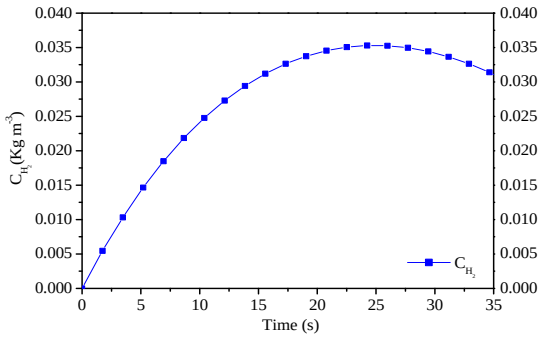

Figure 3: Profile of the chemical species H_2 over time variable under the following operating conditions: Q_g = $1.367x10^{-6}\ m^3\ s^{-1}$ and T = 800°C.

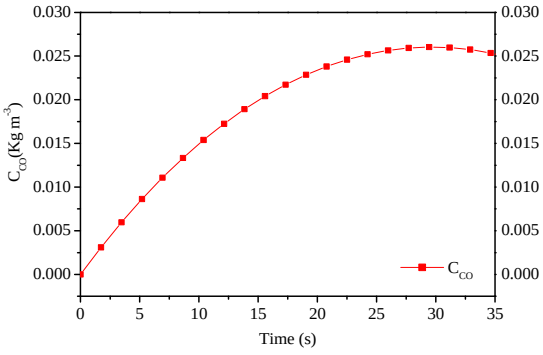

Figure 4: Profile of the chemical species CO over time variable under the following operating conditions: Q_g = 1.367x10-6 $m^3\ s^{-1}$ and T = 800°C.

Figures 3 and 4 show the production of chemical species H_2 and CO, respectively, under the operating conditions adopted. In Figure 3 it can be observed the increase in H_2 concentration over ± 25 s until the

maximum value and then beginning to decrease. In Figure 4 it can be observed the increase in CO concentration which reaches its maximum value to ± 30 s, and then beginning to decrease.

Figures 5 and 6 show the concentrations of the compounds H_2 and CO for different temperature values over time variable. Figure 5 illustrates the results obtained from the study of temperature effect on the H_2 concentration under the conditions described. For the temperature of 800°C is observed the behavior already described in Figure 3. For temperatures of 780°C and 760°C, the concentration of H_2 reached the maximum value in ± 30 s and then starts to decrease. For temperatures of 740°C and 720°C is observed a steady state tendency H_2 production trend from 35 s of reaction. Figure 6 illustrates the results obtained from the study of temperature effect on the CO concentration under the conditions described. For the temperature of 800°C is observed the behavior already described in Figure 4. For the temperature of 780°C, the concentration of CO reached the maximum value in ± 30 s and then starts to decrease. For temperatures of 760ºC, 740ºC and 720°C is observed a steady state tendency CO production trend from 35 s of reaction.

It was performed a more detailed study in order to determine the optimized temperature to run the process. The figures 7 and 8 show the improvement of the yield for the products, H_2 and Co respectively, of the reaction with the temperature varying for every five degrees within the range of steady state tendency determined from the studies shown in figures 5 and 6. From the figure 7 we can notice that the yield of H_2 increases until reaches it's highest value when the temperature is 740°C. From the figure 8 it's possible to conclude that the highest value of yield for the CO is obtained when the temperature is 760°C.

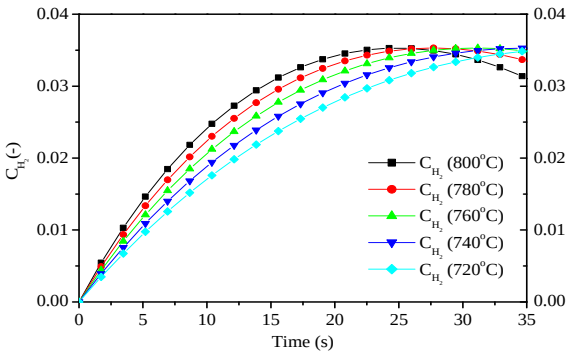

Figure 5: Study of concentration of H_2 under the temperature effects over time variable when Q_g = 1.367x10^{-6} m^3 s^{-1}.

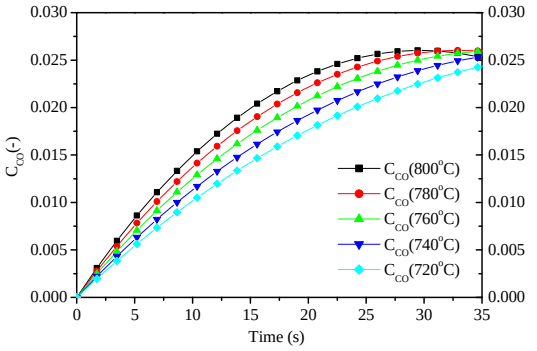

Figure 6: Study of concentration of CO under the temperature effects over time variable when Q_g = 1.367x10^{-6} m^3 s^{-1}.

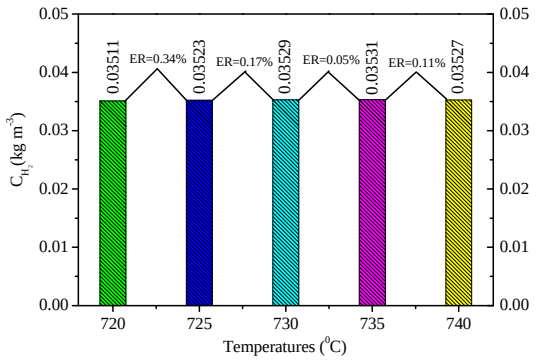

Figure 7: Range of temperature for H_2 production when Q_g = 1.367x10^{-6} m^3 s^{-1}.

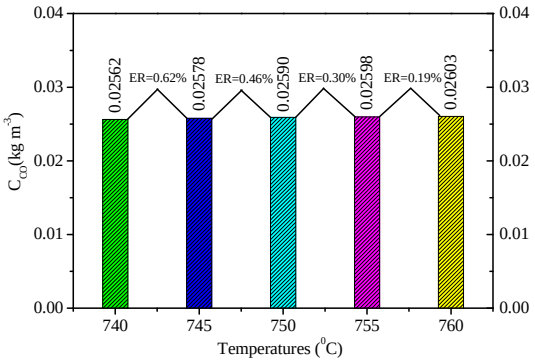

Figure 8: Range of temperature for CO production when Q_g = 1.367x10^{-6} m^3 s^{-1}.

Figures 9 and 10 show the performance of the study for the production of H_2 and CO for temperatures of 800ºC and 730ºC, respectively. In Figure 9 is observed increased income for H_2 production peaking in ± 25 s and then beginning to decline. The yield of CO production grows to the maximum value in ± 30 s and then starts to decrease. In Figure 10 both yield of H_2 as the CO increase to show a tendency to stabilize from 35 s.

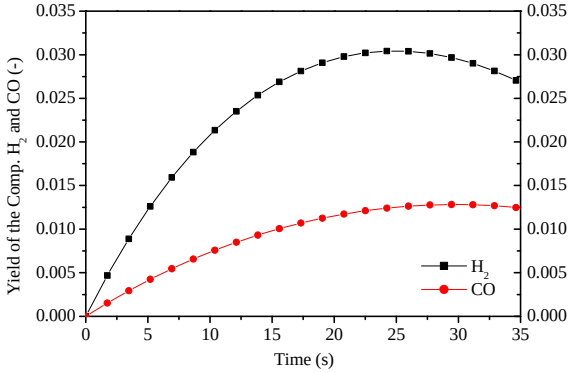

Figure 9: Yield of the chemical species H_2 and CO over time variable when T = 800 °C and Q_g = 1.367x10^{-6} m^3 s^{-1}.

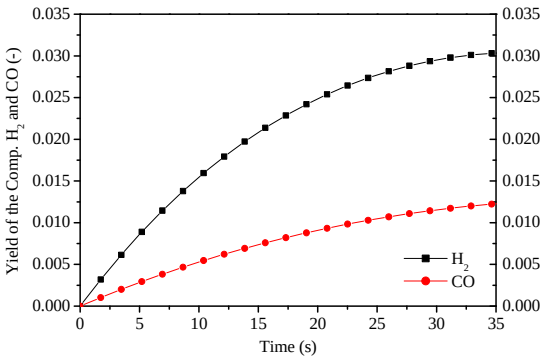

Figure 10: Yield of the chemical species H_2 and CO over time variable when T = 730 °C and Q_g = 1.367x10^{-6} m^3 s^{-1}

4. Conclusions

The model developed for the catalytic reactor FB led to calculations of optimized concentrations of chemical species C_7H_8, O_2, H_2 and CO. The concentration of the chemical species C_7H_8 (toluene) was used to perform the validation of the comparative results of this study and the results obtained by Zhang et al. (2007). For the operating conditions adopted it's possible to obtain a stable production of H_2 and CO in +- 35 s. For variable temperature it's possible verify that, for the chemical specie H_2, the optimum range of operation is between 720°C and 740°C, and the best temperature to get the highest yield is at 740°C, under the adopted operating conditions. For the CO this range is between 720°C and 760°C, and the best temperature to get the highest yield is 760°C. For the chemical species produced, H_2 and CO, under the operating conditions used in this work, and to obtain the highest possible return for both species simultaneously, the process should be carried out at 730°C, temperature which shows the income stabilization trend.

References

Benedito, T. H. S., 2012. Collection, analysis and catalytic degradation of tar produced in acai core gasification and rice husk. PhD Thesis, National Institute for Space Research.

Oliveira, A. A. N., 2012. Mathematical Modeling of the Steam Reforming of Toluene for Fuel Gas Production in a Fixed Bed Catalytic Reactor. PhD Thesis, University of Pernambuco.

Quitete C. P. B., Souza M. M. V. M., 2014, Removing the tar biomass gasification streams: processes and catalysts, New Chemistry, 37, 689-698.

Silva J. D., 2013, Application of Laplace Transform for a Gas-Liquid-Solid Trickle Bed Reactor by Using the Tracer Technique, Applied Mathematics, 4, 167-176.

Simell P., Kurkela E., Stahlberg P., 1996, Hepola J., Catalytic hot gas cleaning of gasification gas, Catalysis Today, 27, 55-62.

Swierczynski D., Courson C., Kiennemann., 2007, A Study of steam reforming of toluene used as model compound of tar produced by biomass gasification, Chemical Engineering and Processing, 47, 508-513.

Zhang R., Wang Y., Brown R. C., 2007, Steam reforming of tar compounds over Ni/olivine catalysts doped with CeO_2, Energy Conversion e Management, 48, 48-68.